

# Calibration Of Parametric Acoustic Array

Chuang Shi, Woon-Seng Gan, and Yong-Kim Chong

School of Electrical and Electronic Engineering  
Nanyang Technological University  
Singapore

shic0002@e.ntu.edu.sg; ewsgan@ntu.edu.sg; eykchong@ntu.edu.sg

**Abstract**— The parametric acoustic array can generate highly directional sound beam by taking advantage of the nonlinear effect in air. The directivity of the sound beam can be controlled by applying phased array techniques, which have been proven to be adequate both in theory and experiment. However, significant mismatches are observed between the theoretical beampatterns and the measured directivities due to the system errors incurred at different stages of implementation. In this paper, we propose a beamsteering structure for the parametric acoustic array that compensates for four types of system errors, namely, the delay error, the weight error, the spacing error, and the wavenumber error. These system errors can be reduced by using a combined optimization approach of Monte Carlo method and nonlinear least squares method. Experimental results are presented to show the feasibility of this proposed beamsteering structure and the optimization approach.

**Keywords**- Array signal processing; Monte Carlo methods; least squares methods; nonlinear acoustics

## I. INTRODUCTION

The discovery and explanation of parametric array effect underwater can be traced back to 1960 when Westervelt [1] first observed the generation of low-frequency wave (also known as the difference frequency wave) through interaction of high-frequency waves (also known as the primary frequency waves). Thereafter, Bennett and Blackstock [2] experimentally observed parametric array effect in air. Until 1983, Yoneyama et al. [3] introduced the parametric array loudspeaker that can create a directional audio beam in air by amplitude modulating a high intensity ultrasonic carrier signal with audible signal. More recently, researchers [4] are experimenting with different usages and techniques of beamsteering the directional sound and achieving a controllable audio beam. In one of the applications, Tanaka et al. [5] implemented an active noise control system with steerable parametric acoustic array to track the moving target.

The digital beamsteering approach proposed by Gan et al. [6] employed the phased array technique to control the beampatterns of the primary frequency waves so as to adjust the directivity of the difference frequency wave (i.e. audible sound beam). This beamsteering capability was based on the theoretical study of scattering of sound by sound carried out by Darvennes et al. [7]. They showed that the audible difference frequency wave can be generated from two non-collinear Gaussian beams based on the nonlinear parabolic wave equation. When the two Gaussian beams are restricted to

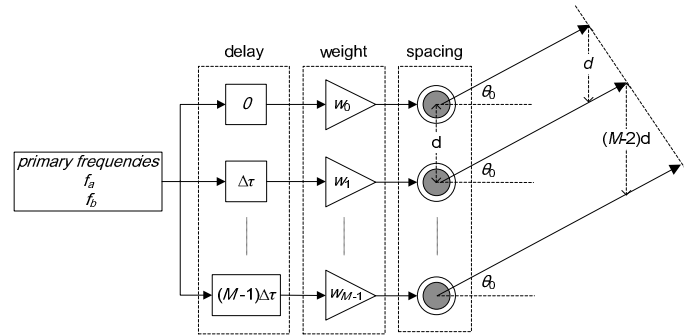


Figure 1. Beamsteering structure of the parametric acoustic array applying phased array technique.

moderate sources separations and interaction angles, the far-field directivity of the difference frequency wave is given by the product of the primary beam directivities.

Previous studies on beamsteering of the parametric acoustic array were mainly based on simulations. However, in a recent publication, Shi et al. [8] have verified the beamsteering capabilities of the parametric loudspeaker with two different transducer array configurations. These array configurations are achieved by grouping transducers into several channels and applying delay-and-sum approach to control the directivity of primary frequency waves. Certain discrepancies were observed between the theoretical beampatterns and the directivities measured in experiment at primary frequencies. The mismatch is significant between the measured difference frequency's directivity and the theoretical beampattern which is computed from the product of the measured directivities of the two primary frequency waves. In this paper, we propose a structure of the steerable parametric acoustic array that takes the system errors into account. Based on the proposed structure, a combined optimization approach of Monte Carlo method and nonlinear least squares method is employed to calibrate the parametric acoustic array. The comparison between measured directivities and calibrated beampatterns by simulations shows significant reduction in matching error.

This paper is organized as follows. The beamsteering structure taking system errors into account is proposed in Section 2. The calibration method of the parametric acoustic array is described in Section 3. In Section 4, the measured directivities are compared with the calibrated beampatterns by simulations. Section 5 concludes the main findings in this paper.

## II. BEAMSTEERING STRUCTURE OF PARAMETRIC ACOUSTIC ARRAY

Based on the product directivity principle, the directivity of the difference frequency wave can be controlled by adjusting the directivity of the primary waves. A fundamental structure of the beamsteerer used in the parametric acoustic array is shown in Fig. 1. The total number of channels is denoted as  $M$ . Assuming that the ultrasonic transducer array is steered to the same direction and shares the same group of weights for the primary frequency waves, thus, the difference frequency wave is also steered to that direction.

According to phased array technology, the increment of delay amounts between adjacent channels is given by

$$\Delta\tau = \frac{d}{c} \sin \theta_0, \quad (1)$$

where  $d$  is the spacing between channels in the ultrasonic transducer array;  $c$  is the sound speed; and  $\theta_0$  is the steering angle of the ultrasonic transducer array. Thus, the far-field beampattern of the steered ultrasonic transducer array for the primary frequency wave is given by

$$H(k, \theta) = \sum_{m=0}^{M-1} w_m \exp\{jmdk(\sin \theta - \sin \theta_0)\}, \quad (2)$$

where  $w_m$  are the weights of channels for  $m = 0, 1, 2, \dots, M-1$ ;  $k$  is the wavenumber of the transmitted primary frequency wave;  $\theta$  is the incidence angle that can range from  $-90^\circ$  to  $90^\circ$ .

Based on the product directivity principle, the far-field directivity of the difference frequency wave  $D_{diff}(\theta)$  is given by

$$D_{diff}(\theta) = H(k_a, \theta) H(k_b, \theta), \quad (3)$$

where  $k_a$  and  $k_b$  are the wavenumbers of primary frequencies  $f_a$  and  $f_b$ , respectively. We always assume that  $f_a < f_b$ , without loss of generality. Thus, the difference frequency wave generated from the two primary frequency waves is given by  $f_{diff} = f_b - f_a$ .

However, in a practical ultrasonic transducer array, there are uncertainties in the locations of the transducers that may change the array configuration from the assumed uniformly distributed one. The weight (or gain) and the delay (or phase) may also be distorted due to the static and dynamic nature of the transducers' characteristics and environmental conditions [9].

In this paper, all the errors involved in the steerable parametric acoustic array are treated as system errors, and classified into four types, namely, the delay error, the weight error, the spacing error, and the wavenumber error. The delay error is incurred, because the phase responses of different channels are not identical to each other. This creates unknown delay increment in each channel in addition to the steering delays. The weight error is generated from the variation of the transducer's and amplifier characteristics in each channel. The quantization error introduced by a typical 16-bit analog output board is relatively small, and can be absorbed into the weight error in this investigation. The spacing error is a common problem found in sensor and transducer arrays, which can be

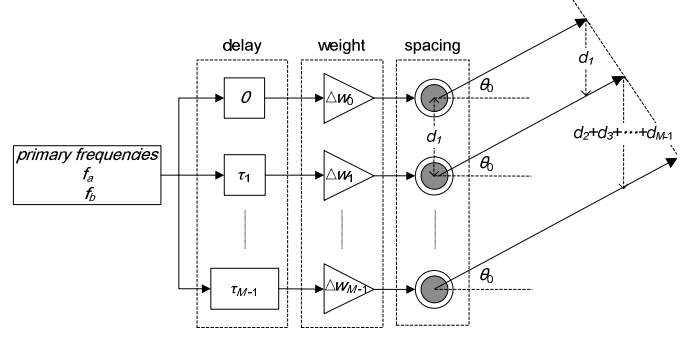


Figure 2. Proposed beamsteering structure of the parametric acoustic array taking system errors into account.

solved by conventional array calibration techniques designed for antenna arrays [9]. The wavenumber error comes from the inaccurate measurement of sound speed and frequency of the primary wave. The beamsteering structure of the parametric acoustic array, which includes the above mentioned system errors, is shown in Fig. 2.  $\tau_i$  is the distorted delay amount of the  $i$ th channel,  $i = 0, 1, 2, \dots, M-1$ ;  $w_i$  is the weight for the  $i$ th channel;  $\Delta w_i$  is the distorted weight of the  $i$ th channel;  $d_i$  is the spacing between channels.

Taking the system errors into account, the beampattern of the primary frequency wave is given by

$$\tilde{H}(k, \theta) = \sum_{m=0}^{M-1} \delta_w^m w_m \exp\{j\delta_D^m m d \delta_K k (\sin \theta - \delta_p^m \sin \theta_0)\}, \quad (4)$$

where  $\delta_w^m$  is the weight distortion factor, representing the distortion of weight for the  $m$ th channel,  $\Delta w_m = \delta_w^m w_m$ ;  $\delta_D^m$  is the spacing distortion factor, representing the distortion of spacing for the  $m$ th channel,  $\delta_D^m m d = \sum d_i$ ;  $\delta_K$  is the wavenumber distortion factor, representing the distortion of wavenumber; and  $\delta_p^m$  is the phase distortion factor, representing the distortion of phase for the  $m$ th channel. Thus, the distorted delay amount of the  $m$ th channel is given by

$$\tau_m = \frac{\delta_D^m m d}{c} \delta_p^m \sin \theta_0. \quad (5)$$

## III. CALIBRATION METHOD OF PARAMETRIC ACOUSTIC ARRAY

In (4), there is one weight distortion factor, one spacing distortion factor and one phase distortion factor per channel. Furthermore, since  $\delta_K$  is a constant, it can always be absorbed into the spacing distortion factor  $\delta_D^m$ . Thus, there are a total of  $3M$  unknown factors.

The calibration of the parametric acoustic array is based on the beamsteering structure with system errors, as shown in Fig. 2. The unknown distortion factors are estimated for minimizing the overall distortion between the measured directivity  $H_m$  with the theoretical beampattern of the primary frequency given by (4). This procedure can be described as

$$\left[ \delta_w^m, \delta_K, \delta_D^m, \delta_p^m \right] = \arg \min_{\theta} \left| H_m(k, \theta) - \tilde{H}(k, \theta) \right|^2. \quad (6)$$

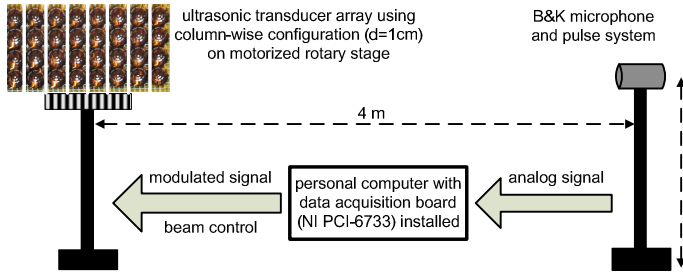


Figure 3. The setup of the transducer array with column-wise configuration and the microphones used in the experiments.

TABLE I. The weight distortion factor and the product of the spacing distortion factor and the wavenumber distortion factor for the  $m$ th channel.

Channel	$\delta_w^m$	$\delta_K \delta_D^m$
1	1.009119039	0.952733887
2	1.002568067	1.086147838
3	0.926929712	0.951851803
4	0.960615335	1.069873776
5	1.146510811	0.95525765
6	1.002047794	1.029496176
7	1.056788515	1.099239352
8	1.029965347	1.089289852

However, the spacing distortion factors and the weight distortion factors are independent from the frequency, and the phase distortion factors are related with frequency. Thus the frequency-dependent and frequency-independent factors have to be solved separately. Hence, we introduce a combined optimization approach of the Monte Carlo method and nonlinear least squares method.

First, an initial estimation of the spacing distortion factors and the weight distortion factors are generated from random vector generator with uniform distribution between 0.85 and 1.15. This range is observed from experiments. Second, based on the randomly generated guesses, the phase distortion factors can be solved by the nonlinear least squares method. PSNR (peak signal to noise ratio) is utilized to evaluate the mismatch between the theoretical beampatterns and the beampatterns measured in experiment that can be given by the residuals of the nonlinear least square solution. In this case, the measured beampatterns are the original signal and the theoretical beampatterns are the noisy approximation of the original signal. We express the PSNR values for various primary frequencies in terms of the logarithmic decibel scale. To improve the PSNR values, (i.e. to get a more accurate calibration data), more samples of the weight distortion factors and the spacing distortion factors are apparently demanded. The calibrating procedure can be done iteratively, and the termination condition occurs when the improvement of the overall PSNR is less than 1 dB in the past 10000 randomly generated samples.

#### IV. MEASUREMENTS

The beampatterns of the primary waves and the difference frequency waves were measured in an anechoic chamber with a dimension of 6 m  $\times$  3 m  $\times$  3 m. The primary waves were captured by an 1/8 inch microphone (B&K 4138). The

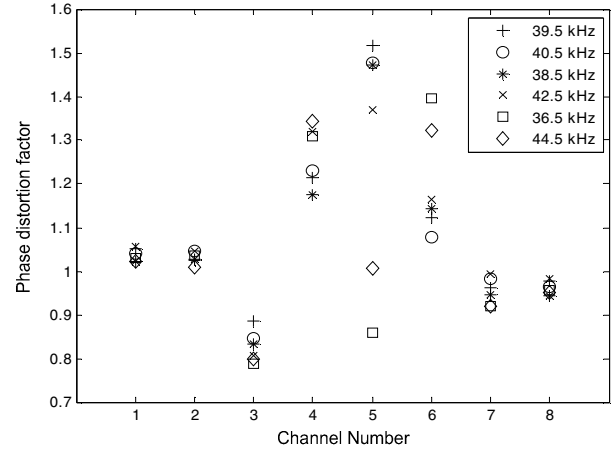


Figure 4. The phase distortion factor for the  $m$ th channel at different primary frequencies.

TABLE II. PSNR comparison between the structures without system error and with system error at various frequencies

Freq. (kHz)	Structure in Fig.1 (dB)	Structure in Fig.2 (dB)	Improvement after calibration
39.5	17.0970	25.1766	8.0796
40.5	18.1250	25.7453	7.6203
1.0	8.7094	10.3000	1.5906
38.5	17.2672	23.0712	5.804
42.5	16.0315	25.3317	9.3002
4.0	10.2592	10.4276	0.1684
36.5	14.7317	23.4780	8.7463
44.5	13.3258	21.9590	8.6332
8.0	12.8646	14.2970	1.4324

difference frequency waves were measured using a 1/2 inch microphone (B&K 4134). The ultrasonic transducer array was configured in column-wise, as shown in Fig. 3. The ultrasonic transducer array was mounted on a motorized rotation stage, and the microphones were placed at a location 4 meters away from the center of the ultrasonic transducer array. Fig. 3 also shows the overall setup of the measurements. The beampatterns of the primary frequency wave, as well as the difference frequency wave were restricted to a measuring angle of  $-40^\circ$  to  $40^\circ$  with a resolution of  $1^\circ$ . All the channels in the ultrasonic transducer array were equally weighted, but differently delayed to achieve beamsteering. A beamsteering algorithm was carried out in a data acquisition board (NI PCI-6733).

By the combined optimization approach of Monte Carlo method and nonlinear least squares method, the weight distortion factors  $\delta_w^m$  and the spacing distortion factors  $\delta_K \delta_D^m$  are solved and the results are shown in Table 1. The phase distortion factors  $\delta_p^m$  are solved for primary frequencies at 36.5 kHz, 38.5 kHz, 39.5 kHz, 40.5 kHz, 42.5 kHz and 44.5 kHz. The results of  $\delta_p^m$  are plotted in Fig. 4.

Table 2 shows the PSNR values at 6 primary frequencies and their corresponding difference frequencies before and after calibration. The theoretical beampatterns of the difference frequency waves are obtained based on the product directivity principle [7]. In the PSNR comparison, the beamsteering

## V. CONCLUSION

In this paper, we proposed a beamsteering structure of the parametric acoustic array that takes into account four types of system errors. Based on the proposed beamsteering structure and measured beampatterns at primary frequencies, a combined optimization approach of Monte Carlo method and nonlinear least squares method was proposed to solve the calibration equation of the parametric acoustic array. The experimental results showed significant improvement in matching between the theoretical beampattern and the measured directivity at the primary frequency. At the difference frequency, where the error caused from product directivity principle is dominating, the performance of the proposed calibration approach is limited. However, the accuracy of predicting locations of grating lobes can be improved when using the proposed beamsteering structure, which is of importance to provide better grating lobe elimination [8] when designing steerable parametric acoustic array.

## ACKNOWLEDGMENT

This work is partially supported by the Singapore National Research Foundation Interactive Digital Media R&D Program, under research grant NRF2007IDM-IDM002-086; and the Singapore Ministry of Education Academic Research Fund Tie-2, under research grant MOE2010-T2-2-040.

## REFERENCES

- [1] P. J. Westervelt, "Parametric acoustic array," *J. Acoust. Soc. Am.*, vol. 35, no. 4, pp. 535-537, 1963.
- [2] M. B. Bennett and D. T. Blackstock, "Parametric array in air," *J. Acoust. Soc. Am.*, vol. 57, no. 3, pp. 562-568, 1975.
- [3] M. Yoneyama and J. Fujimoto, "The audio spotlight: An application of nonlinear interaction of sound waves to a new type of loudspeaker design," *J. Acoust. Soc. Am.*, vol. 73, no. 5, pp. 1532-1536, 1983.
- [4] C. Shi and W. S. Gan, "Development of parametric loudspeaker: a novel directional sound generation technology," *IEEE Potentials*, vol. 29, no.6, pp. 20-24, 2010.
- [5] N. Tanaka and M. Tanaka, "Active noise control using a steerable parametric array loudspeaker," *J. Acoust. Soc. Am.*, vol. 127, no. 6, pp. 3526-3537, 2010.
- [6] W. S. Gan, J. Yang, K. S. Tan, M. H. Er, "A digital beamsteerer for difference frequency in parametric array," *IEEE Trans. Audio Speech Lang. Process.*, vol. 14, no. 3, pp. 1018-1025, May 2006.
- [7] C. M. Darvennes and M. F. Hamilton, "Scattering of sound by sound from two Gaussian beams," *J. Acoust. Soc. Am.*, vol. 87, no. 5, pp. 1955-1964, 1990.
- [8] C. Shi and W. S. Gan, "Grating lobe elimination in steerable parametric loudspeaker," *IEEE Trans. Ultrason. Ferroelectr. Freq. Control*, vol. 58, no. 2, pp. 437-450, 2011.
- [9] D. H. Johnson and D. E. Dudgeon, *Array Signal Processing: Concepts and Techniques*, New Jersey: Prentice Hall, 1993.

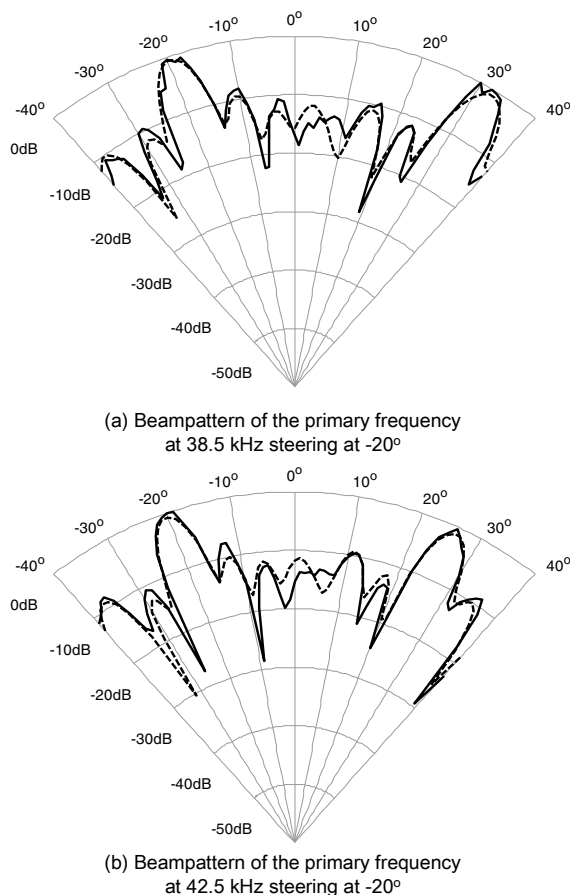


Figure 5. The comparison of the measured directivities (solid line) and the simulated beampatterns using structure in Fig.2 (dash line) at primary frequencies.

structure with calibration of system errors (in Fig. 2) results in 8 dB better than the beamsteering structure without calibration (in Fig. 1) at the primary frequencies on average. However, at the difference frequencies, the PSNR values are only slightly improved by applying the beamsteering structure with system errors. Since the product directivity principle is an approximate result of the second-order wave equation with limitations [7], the mismatch between the theoretical beampattern and the measured directivity at the difference frequency is mainly contributed by the nonlinear acoustics model instead of system errors.

Fig. 5 compares the measured directivities and the simulated beampatterns using structure shown in Fig.2. At both the primary frequencies, within in beamwidths of the first and the second sidelobes adjacent to the mainlobe or the grating lobe, accurate matches are observed.